

A Grid-based Adaptive Scheme for the Three-Dimensional Forging and Extrusion Problems with the EFG Method

H. S. Lu and C. T. Wu

Livermore Software Technology Corporation

Livermore, CA 94551

hslu@lstc.com, ctwu@lstc.com

Abstract

Procedures to adaptively refine meshes are emerging as an important tool for improving accuracy and efficiency in large deformation and fracture analysis. Comparing to the mesh-based adaptive method, the grid-based adaptive mesh-free method has several built-in advantages including naturally conforming in shape functions, smoothed interpolations in surface construction and state variable transfer, and the results are less sensitive to the unstructured grids. In this paper, a grid-based adaptive scheme is proposed for the Element Free Galerkin method in the large deformation analysis of three-dimensional forging and extrusion simulations. To precisely account for the effect of kernel functions during adaptive procedure, we consider the meshfree adaptivity in the framework of arbitrary Lagrangian-Eulerian meshfree method with an operator-split time integration. A grid-based interpolation scheme adopted from the meshfree approximation is developed for the state variable transfer after mesh refinement to improve conservation and monotonic properties. Several industrial problems have been solved and compared to the existing numerical methods.

1. Introduction

Adaptive procedure has become an important tool for structural analysis, especially in problems with large deformation, moving interface, and local behavior, where the optimal mesh dramatically changes during the deformation process. Several complex issues, such as error indicator, mesh refinement, state variable transfer, are involved in the adaptive procedures. In this work, we mainly address the transfer of state variables between the successive meshes, which is crucially important for preserving the accuracy, convergence properties in solving the problems with history-dependent materials. Several important aspects should be considered for the state variable transfer, such as consistency with the constitutive equations, requirement of equilibrium, compatibility of the state variables at gauss points with the state variables at nodal points, and minimization of the numerical diffusion, etc. Various transfer schemes can be found in the literatures [2, 5, 10, 11] for finite element method. The approaches used in [5, 11] are very similar. The state variables in the old mesh are first projected to nodes, and then the values at new integration points are interpolated from the old mesh. A different approach is proposed in [10]. The state variables are transferred from old gauss points to the new gauss points by local interpolation function. This direct transfer does not require nodal projection, but the continuity of state variable along the element boundary is not ensured. Recently developed approximation theories such as moving least square approximation (MSL) [1], reproducing kernel approximation (RKPM) [8] allow the interpolation functions to be constructed entirely in terms of arbitrarily placed nodes without the used of an element connectivity. This makes the direct transfer of information between the subsequent meshes with a desirable consistency and accuracy possible, especially in the direct transfer of state variable at integration point during the adaptive procedure. In this work, a local interpolant with a desirable consistency condition,

which is based on the modified moving-least squares approximation (or the modified reproducing kernel approximation), is constructed to obtain the state variables at new integration points from old integration points.

Recent developments in mesh-free methods add an additional dimension to computational mechanics [1, 3, 8, 14, 15]. Those methods do not rely on the conventional grid approach to define approximation functions. In comparison with conventional finite element methods, the characteristics of smoothness and naturally conforming of the approximation, exemption from meshing, and higher convergence rate and the easy of nodal insertion and deletion have make mesh-free methods attractive alternative numerical techniques for nonlinear analysis of industrial applications. Although mesh-free method has been extensively investigated and applied to large deformation analysis in the past few years [1, 3, 6], its application to forging and extrusion problems that are beyond the Lagrangian description is still a challenging problem due to the issues in moving surface representation, volumetric locking and domain integration. In this work we take the meshfree adaptivity [9, 13, 15] in the framework of arbitrary Lagrangian-Eulerian meshfree method [12]. By doing so, the adaptive procedure is separated into kernel function redefining due to the material deformation and mesh refinement based on the error indicator. An advection algorithm is employed to account for the effect of kernel function change in the adaptive procedure. The refinement of grids is accomplished by a delaunay-type algorithm with a grid distance control. A special mesh-free interpolation is used to build a complete three-dimensional geometric and topologic representation to preserve the volume during the adaptive procedure.

The layout of this paper is as follows. In section 2, moving least square approximation, one of the most popular meshfree approximations, is reviewed. Meshfree adaptivity with adaptive Lagrangian particles and Eulerian kernel is discussed in Section 3. In section 4, the transfer of state variables between the subsequent meshes is presented. Two numerical examples are given in Section 4.

2. Meshfree Approximation

The discrete moving least square (MLS) approximation of a function $u(\mathbf{x})$, denoted by $u^h(\mathbf{x})$, is constructed by a combination of the monomials as

$$u^h(\mathbf{x}) = \sum_{i=1}^n H_i(\mathbf{x})b_i(\mathbf{x}) \equiv \mathbf{H}^T(\mathbf{x})\mathbf{b}(\mathbf{x}) \quad (1)$$

where n is the order of completeness in this approximation, the monomial $H_i(\mathbf{x})$ are basis functions, and $b_i(\mathbf{x})$ are the coefficients of the approximation.

The coefficients $b_i(\mathbf{x})$ at any point \mathbf{x} are depending on the sampling points \mathbf{x}_I that are collected by a weighting function $w_a(\mathbf{x} - \mathbf{x}_I)$. This weighting function is defined to have a compact support measured by 'a', i.e., the sub-domain over which it is nonzero is small relative to the rest of the domain. Each sub-domain $\Delta\Omega_I$ is associated with a node I . The most commonly used sub-domains are disks or balls.

In this development, we employ the cubic B-spline kernel function as the weighting function:

$$w_a(\mathbf{x} - \mathbf{x}_I) = \begin{cases} \frac{2}{3} - 4\left(\frac{\|\mathbf{x} - \mathbf{x}_I\|}{a}\right)^2 + 4\left(\frac{\|\mathbf{x} - \mathbf{x}_I\|}{a}\right)^3 & \text{for } 0 \leq \frac{\|\mathbf{x} - \mathbf{x}_I\|}{a} \leq \frac{1}{2} \\ \frac{4}{3} - 4\left(\frac{\|\mathbf{x} - \mathbf{x}_I\|}{a}\right) + 4\left(\frac{\|\mathbf{x} - \mathbf{x}_I\|}{a}\right)^2 - \frac{4}{3}\left(\frac{\|\mathbf{x} - \mathbf{x}_I\|}{a}\right)^3 & \text{for } \frac{1}{2} < \frac{\|\mathbf{x} - \mathbf{x}_I\|}{a} \leq 1 \\ 0 & \text{otherwise} \end{cases} \quad (2)$$

The moving least-squares technique consists in minimizing the weighted L_2 -Norm

$$J = \sum_{I=1}^{NP} w_a(\mathbf{x} - \mathbf{x}_I) \left[\sum_{i=1}^n H_i(\mathbf{x}) b_i(\mathbf{x}) - u(\mathbf{x}_I) \right]^2 \quad (3)$$

where NP is the number of nodes within the support of \mathbf{x} for which the weighting function $w_a(\mathbf{x} - \mathbf{x}_I) \neq 0$.

Equation (3) can be written in the form

$$J = (\mathbf{H}\mathbf{b} - \mathbf{u})^T \mathbf{W}_a(\mathbf{x})(\mathbf{H}\mathbf{b} - \mathbf{u}) \quad (4)$$

where

$$\mathbf{u}^T = (u_1, u_2, \dots, u_{NP}) \quad (5)$$

$$\mathbf{H} = \begin{bmatrix} \{\mathbf{H}(\mathbf{x}_1)\}^T \\ \dots \\ \{\mathbf{H}(\mathbf{x}_{NP})\}^T \end{bmatrix} \quad (6)$$

$$\{\mathbf{H}(\mathbf{x}_i)\}^T = \{H_1(\mathbf{x}_i), \dots, H_n(\mathbf{x}_i)\} \quad (7)$$

$$\mathbf{W}_a = \text{diag}[w_a(\mathbf{x} - \mathbf{x}_1), \dots, w_a(\mathbf{x} - \mathbf{x}_{NP})] \quad (8)$$

To find the coefficients \mathbf{b} , we obtain the extremum of J by

$$\frac{\partial J}{\partial \mathbf{b}} = \mathbf{M}^{[n]}(\mathbf{x})\mathbf{b}(\mathbf{x}) - \mathbf{B}(\mathbf{x})\mathbf{u} = 0 \quad (9)$$

where $\mathbf{M}^{[n]}(\mathbf{x})$ is called the moment matrix of $w_a(\mathbf{x} - \mathbf{x}_I)$ and is given by

$$\mathbf{M}^{[n]}(\mathbf{x}) = \mathbf{H}^T \mathbf{W}_a(\mathbf{x}) \mathbf{H} \quad (10)$$

$$\mathbf{B}(\mathbf{x}) = \mathbf{H}^T \mathbf{W}_a(\mathbf{x}) \quad (11)$$

So we have

$$\mathbf{b}(\mathbf{x}) = \mathbf{M}^{[n]-1}(\mathbf{x})\mathbf{B}(\mathbf{x})\mathbf{u} \quad (12)$$

For $\mathbf{M}^{[n]}(\mathbf{x})$ to be invertible, the support of $w_a(\mathbf{x} - \mathbf{x})$ needs to be greater than a minimum size that is related to the order of basis functions.

Using the solution of Equations (1), (10), (11) and (12), the EFG approximation is obtained by

$$u^h(\mathbf{x}) = \sum_{I=1}^{NP} \Psi_I(\mathbf{x})u_I \quad (13)$$

where the EFG shape functions $\Psi_I(\mathbf{x})$ are given by

$$\Psi_I(\mathbf{x}) = \mathbf{H}^T(\mathbf{x})\mathbf{M}^{[n]-1}(\mathbf{x})\mathbf{B}(\mathbf{x}) \quad (14)$$

and $\Psi_I(\mathbf{x})$ are n th-order complete, i.e.

$$\sum_{I=1}^{NP} \Psi_I(\mathbf{x})x_{1I}^p x_{2I}^q x_{3I}^r = x_1^p x_2^q x_3^r \quad \text{for } p + q + r = 0, \dots, n \quad (15)$$

In general, mesh-free shape functions Ψ_I do not possess Kronecker delta properties of the standard FEM shape functions, i.e.

$$\Psi_I(\mathbf{x}_J) \neq \delta_{IJ} \quad (16)$$

This means that the coefficients of the interpolant are not the same as the nodal value, i.e.

$$u^h(\mathbf{x}_I) \neq u_I \quad (17)$$

3. Adaptive Lagrangian Particles with Eulerian Kernel

Without using the explicit mesh, meshfree method is more suitable for the adaptive procedure than the conventional finite element method. Particles can be easily added and removed without complications in the data structure. The accuracy and smoothness of meshfree solution reduce the numerical diffusion during the transfer of state variable between the subsequent meshes. Beside the mesh refinement, kernel functions (weighting functions) associated with the particles also need to be redefined in the procedure of adaptivity. To precisely account for the effect of kernel functions, we consider the meshfree adaptivity in the framework of arbitrary Lagrangian-Eulerian meshfree method with an operator-split time integration. As shown in Figure 1, the adaptive procedure is separated as redefining kernel functions in the old mesh due to the material deformation, and mesh refinement to create new mesh.

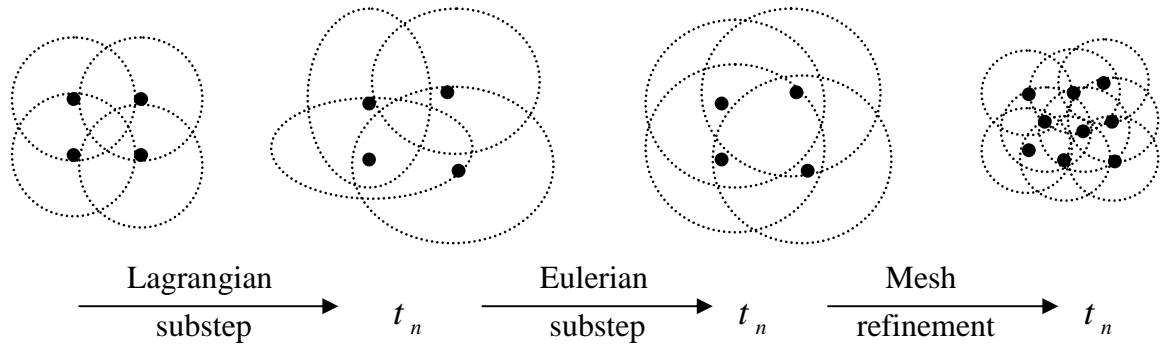


Figure 1 Adaptive Procedure in Meshfree Method

Three coordinates, the Lagrangian or material coordinate \mathbf{X} , the spatial coordinate \mathbf{x} , and the referential coordinate $\boldsymbol{\chi}$, and the three time derivatives of a function f , the material derivative $\dot{f} = \left. \frac{\partial f(\mathbf{X}, t)}{\partial t} \right|_{\mathbf{x}}$, the spatial derivative $\frac{\partial f}{\partial t} = \left. \frac{\partial f(\mathbf{x}, t)}{\partial t} \right|_{\mathbf{x}}$, and the referential derivative $\overset{\circ}{f} = \left. \frac{\partial f(\boldsymbol{\chi}, t)}{\partial t} \right|_{\boldsymbol{\chi}}$ are defined respectively. The relationship between the material and referential time derivative can be written as:

$$\dot{f} = \overset{\circ}{f} + \mathbf{c} \cdot \nabla f = \overset{\circ}{f} + c_i \frac{\partial f}{\partial x_i} \quad (18)$$

Where \mathbf{c} is the relative velocity between the material $\mathbf{v} = \dot{\mathbf{x}}$ and the referential $\hat{\mathbf{v}} = \overset{\circ}{\mathbf{x}}$ velocity.

$$\mathbf{c} = \mathbf{v} - \hat{\mathbf{v}} \quad (19)$$

The referential momentum equation of the transient problem can be written as

$$\sigma_{ij,j} + \rho b_i = \rho(\overset{\circ}{v}_i + c_j v_{i,j}) \quad \text{in } \Omega \quad (20)$$

Where σ_{ij} is the stress field, ρ is mass density, and b_i is the body force. The boundary and initial conditions are given as $u_i = \bar{u}_i$ on Γ_u , $\sigma_{ij} n_j = h_i$ on Γ_h , $u_i(\mathbf{X}, 0) = u_i^0(\mathbf{X})$, $v_i(\mathbf{X}, 0) = v_i^0(\mathbf{X})$, and $\overset{\circ}{v}_i(\mathbf{X}, 0) = \overset{\circ}{v}_i^0(\mathbf{X})$ respectively. The corresponding weak form reads

$$\int_{\Omega} \rho \delta u_i \overset{\circ}{v}_i d\Omega + \int_{\Omega} \rho \delta u_i c_j v_{i,j} d\Omega + \int_{\Omega} \delta u_{i,j} \sigma_{j,i} d\Omega = \int_{\Omega} \rho \delta u_i b_i d\Omega + \int_{\Gamma_h} \delta u_i h_i d\Gamma_h \quad (21)$$

Substituting the meshfree approximation into Equ.(21) to obtain the matrix form

$$\mathbf{M} \dot{\mathbf{v}} + \mathbf{C} \mathbf{v} + \mathbf{K} \mathbf{u} = \mathbf{f}^{ext} \quad (22)$$

Where

$$\begin{aligned} M_{IJ} &= \int_{\Omega} \rho \Psi_I(\chi) \Psi_J(\chi) d\Omega \\ C_{IJ} &= \int_{\Omega} \rho c_j \psi_I(\chi) \psi_{J,j}(\chi) d\Omega \\ K_{IJ} &= \int_{\Omega} \mathbf{B}_I \mathbf{D} \mathbf{B}_J d\Omega \\ f_I^{ext} &= \int_{\Omega} \rho \psi_I(\chi) \mathbf{b} d\Omega + \int_{\Gamma_h} \psi_I(\chi) \mathbf{h} d\Gamma_h \end{aligned} \quad (23)$$

\mathbf{B} is the strain-displacement matrix

An operator-split with a Lagrangian substep followed by an Eulerian substep is adopted to integrate the equations in time if the adaptive procedure is invoked. During the Lagrangian substep, the material and referential coordinate systems are chosen as the same, and the convective velocity \mathbf{c} is trivially zero, i.e. $\mathbf{v} = \hat{\mathbf{v}}$. In the Eulerian substep, the kernel function is redefined due to the current material deformation. The solution variables have to be transferred with an advection algorithm between the same mesh due to the different kernel functions.

$$f = f^{LAG} + \Delta f \Big|_{\chi} \approx f^{LAG} + \mathbf{d} \cdot \nabla f \quad (24)$$

Where \mathbf{d} is the total displacement during the convective step. f^{LAG} is the quantity f from the Lagrangian substep.

Unlike in ALE finite element method, the new state variable value after convection can be naturally obtained due to the smoothness of the shape function by

$$f = f^{LAG} + \mathbf{d} \cdot \left(\sum_I \frac{\partial \psi_I}{\partial \chi} \Big|_{\chi=\chi^{LAG}+\theta \mathbf{d}} f_I \right) \quad (25)$$

Where θ is a parameter between 0 and 1

4. State Variable Transfer

In recent years mesh-free methods has been developed by employing new approximation theories such as moving least square approximation (MSL) [1], reproducing kernel approximation (RKPM) [8] that allow the shape functions to be constructed entirely in terms of arbitrarily placed nodes without the used of an element connectivity in the classical sense. This makes the direct transfer of information between the subsequent meshes with a desirable consistency possible, especially in the direct transfer of state variable at integration point during the adaptive procedure as shown in Figure 2. In this work, a local interpolant with a desirable consistency condition, which is based on the modified meshfree approximation, is constructed to directly obtain the state variables at new integration points from old integration points. The numerical diffusion near the boundary, especially in areas undergoing rapid transients, such as the contact boundary part needs to be limited during state variable transfer. A special treatment with using the smoothness of meshfree approximation is adopted to minimize the effect of the

numerical diffusion. The state variables at nodal and integration points for the new mesh can be interpolated from the old mesh as

$$f(\mathbf{x}) = \sum_{I=1} \hat{\Psi}_I(\mathbf{x}) f_I \quad (26)$$

Where $\hat{\Psi}(\mathbf{x})$ is the modified meshfree approximation functions [3, 4, 7]

As a test problem we take the following equation

$$-\frac{d}{dx} \left(\frac{du}{dx} \right) + u = g \quad \text{on } x \in (0,1) \quad (27)$$

with the boundary conditions $u(0) = u(1) = 0$. By choosing function g such that the exact solution of the problem reads

$$u = x^2 - \frac{\sinh 4x}{\sinh 4} \quad (28)$$

As shown Figures 3 and 4, the recovery solution has the same accuracy and convergence rate as the EFG numerical solution.

5. Numerical Examples

Two forging examples are analyzed by using the proposed adaptive EFG method. The adaptive procedure is triggered by a given time interval, and the grid distribution is controlled by the specific maximum and minimum grid space. Error indicator for adaptive EFG method will be discussed in the other paper.

5.1 Wheel Forging

The wheel forging problem as shown in Figure 5 (a) is first tested by using the Lagrangian EFG method. It can not finish the job because the mesh is too coarse to capture the local behavior in areas undergoing rapid transient. The problem is analyzed by employing the adaptive procedure with increasing nodes from 5827 to 13661. The distribution of effective plastic strain in the final deformation is plotted in Figure 5 (b). During the adaptive procedure, the monotonic property of the internal variables such as the effective plastic strain can be maintained. This is due to the linear consistency of the interpolation function during the state variable transfer. The volume and the reaction force are given in Figures 6 and 7 respectively for EFG method and adaptive EFG method. The adaptive EFG result is comparable with the EFG result.

5.2 Forging of Piston Housing

The piston housing as shown in Figure 8 (a) is simulated in this example. The final deformation with material flash is given in Figure 8 (b). There are two important issues, suck-in defect Figure 9 (a) and material flash Figure 9 (b), in this simulation. To successfully capture suck-in defect in the adaptive simulation, a fine mesh (or a local fine mesh) and an accurate state variable transfer

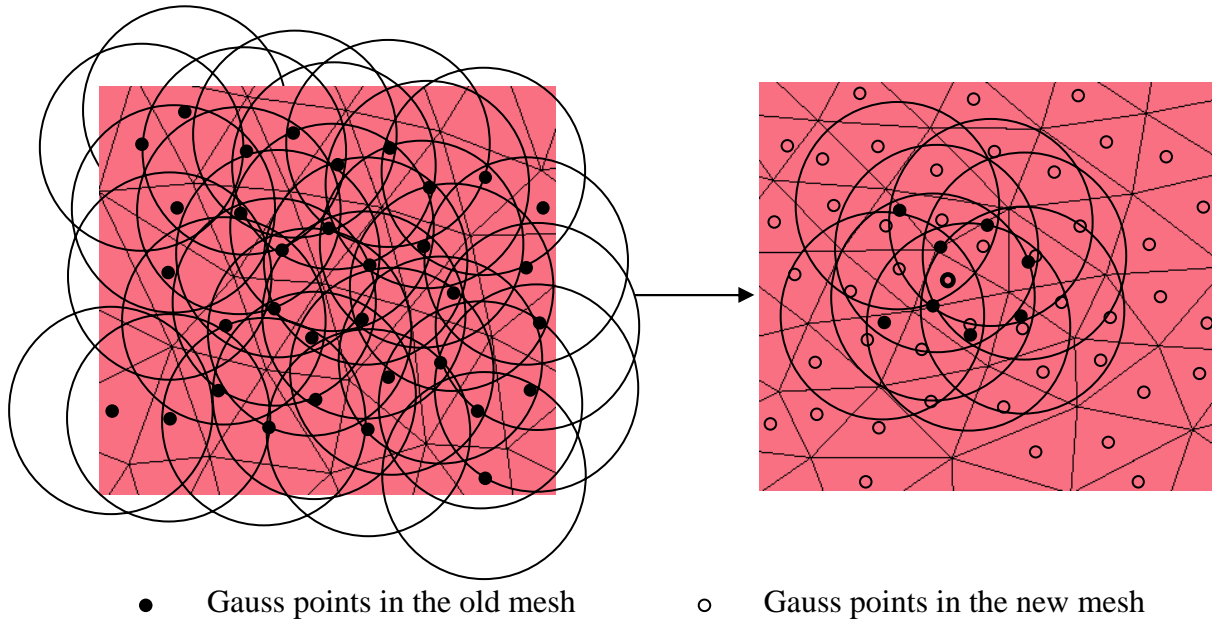


Figure 2 direct state variable transfer between two subsequent meshes

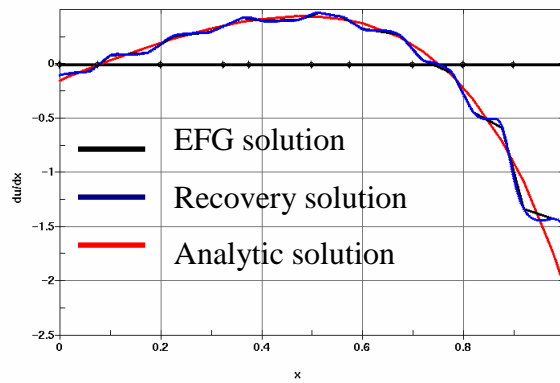


Figure 3 The comparison of numerical, recovery and analytic solutions

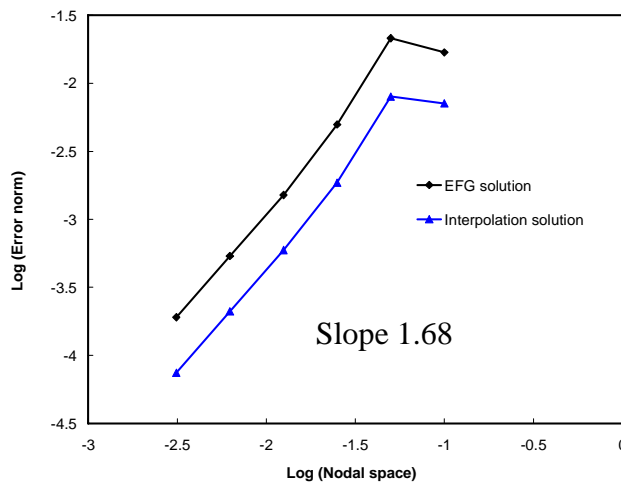
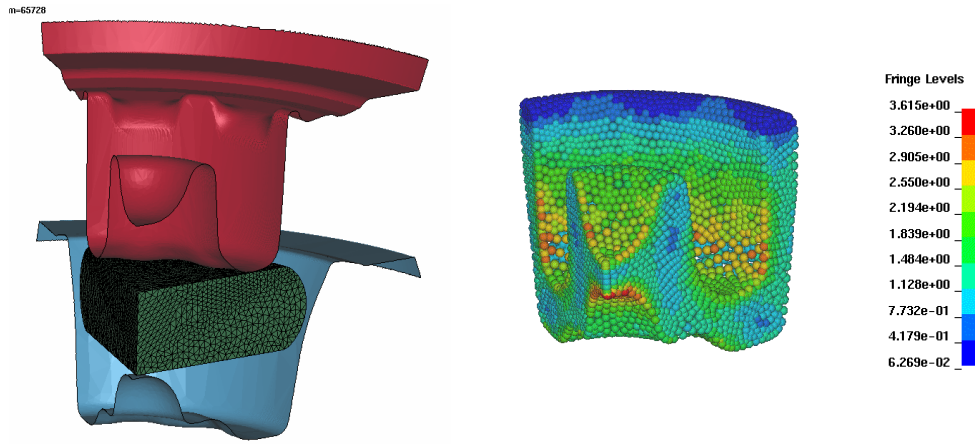


Figure 4 The convergence rate in the first derivative of solution



(a) Problem description

(b) Contour plot of plastic strain

Figure 5 Problem statement and contour plot of plastic strain

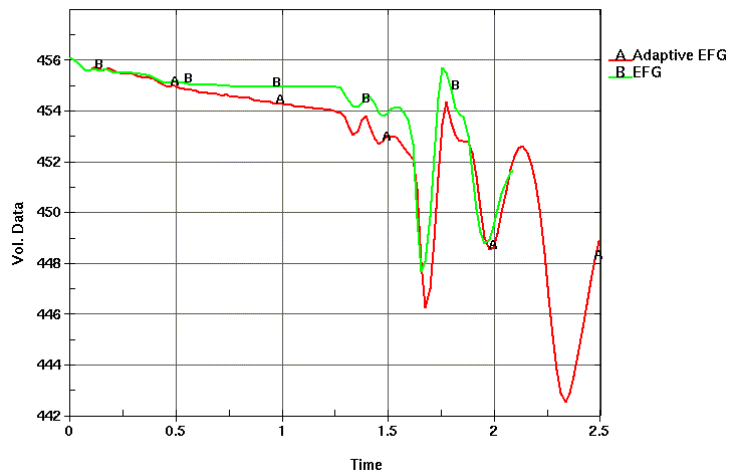


Figure 6 Volume change in the simulation

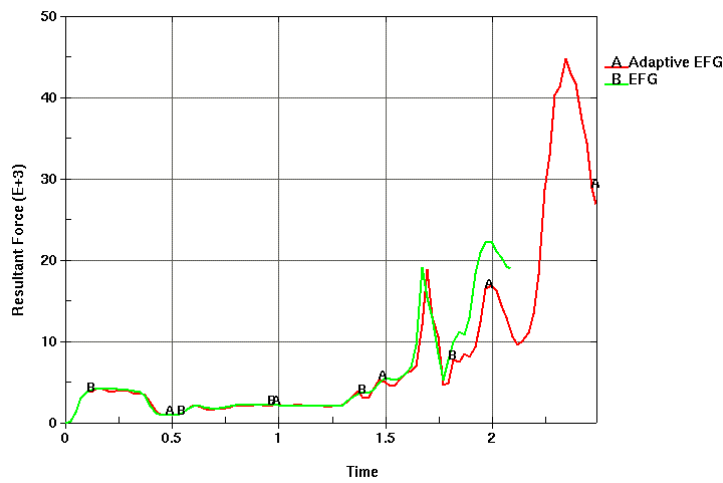
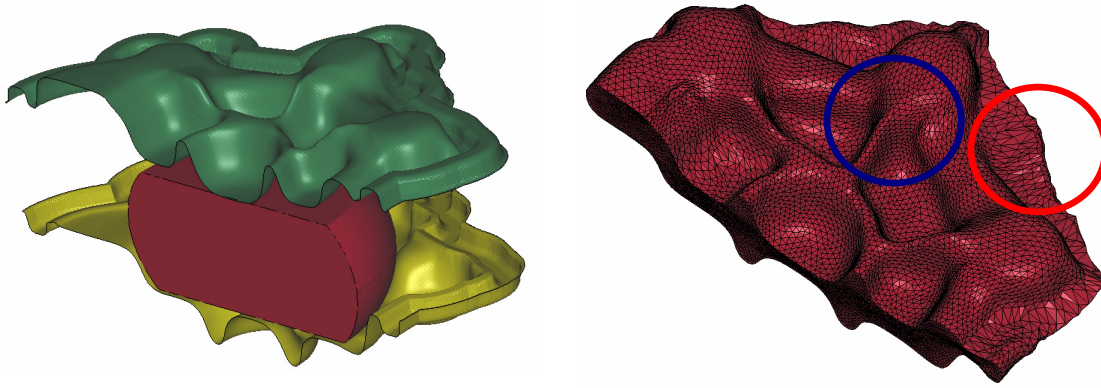


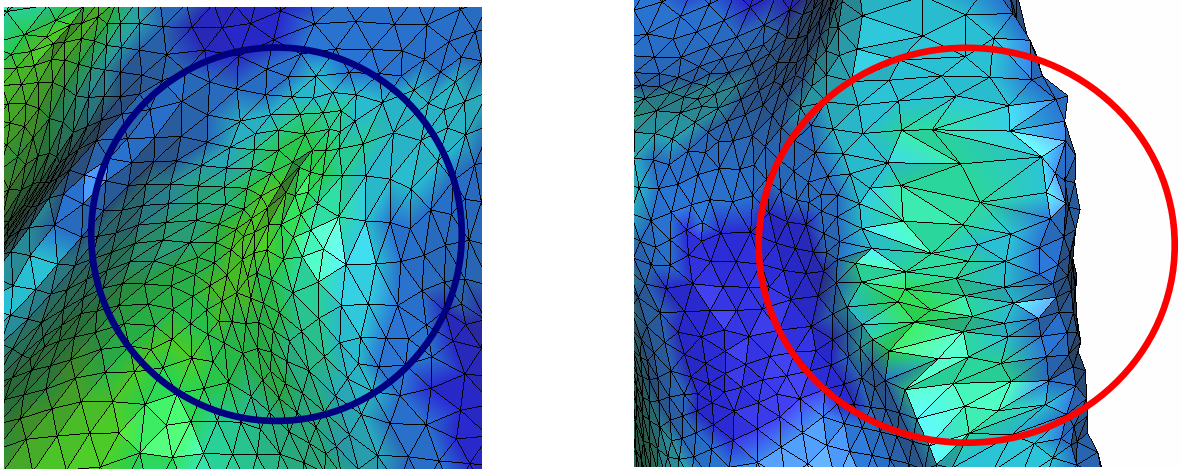
Figure 7 Reaction force



(a) Problem description

(b) Final deformation

Figure 8 Problem statement and final deformation



(a) Suck-in defect

(b) Material flash

Figure 9 Suck-in defect and material flashes

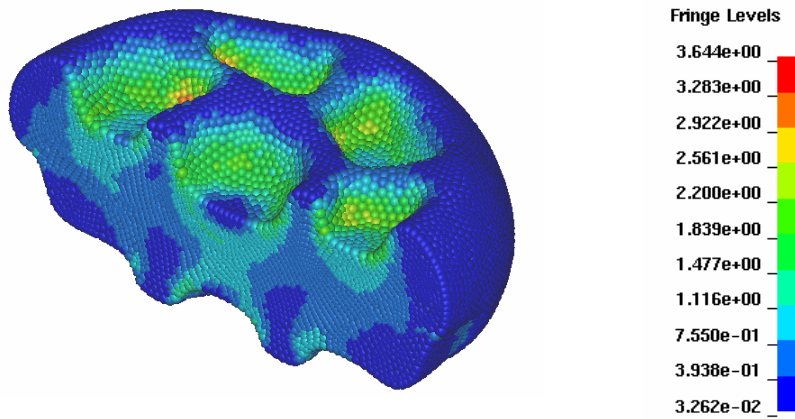


Figure 10 Contour plot of the effective plastic strain

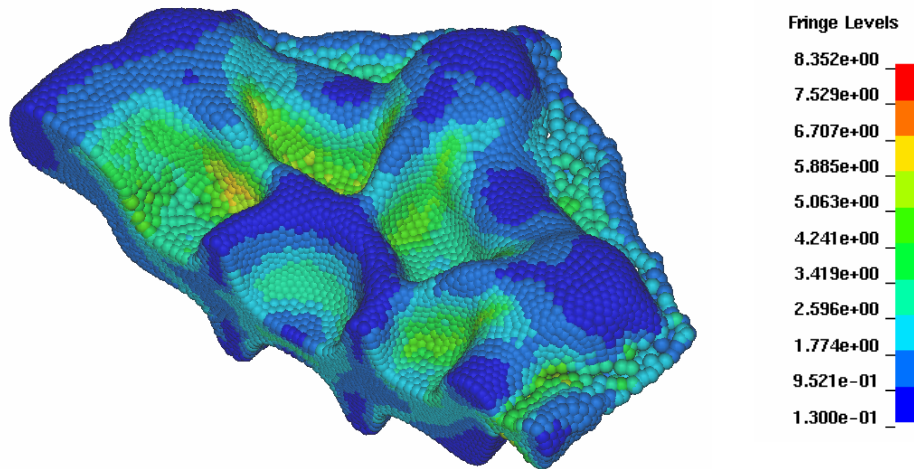


Figure 11 Contour plot of the effective plastic strain

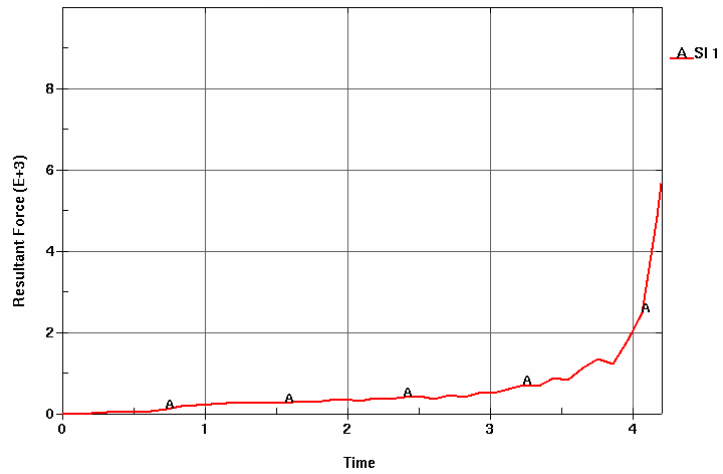


Figure 12 Reaction force

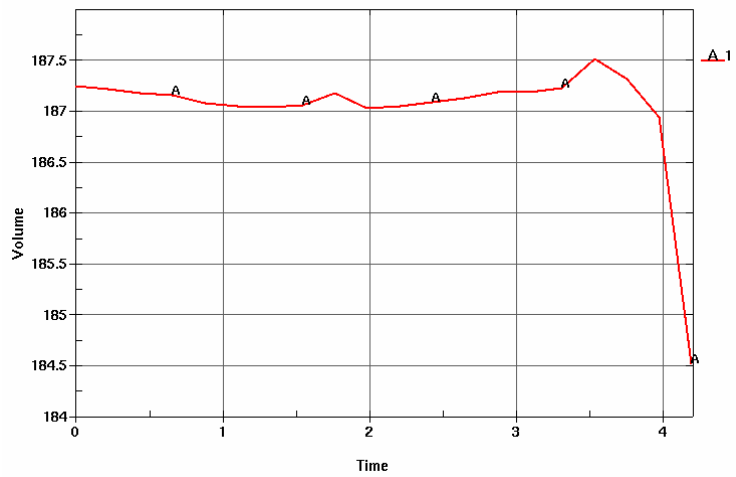


Figure 13 Volume change

are required. The proposed modified meshfree interpolation can effectively transfer the state variables between subsequent meshes without losing the high order information. The improved EFG method can handle the material flash effectively. Figures 10 and 11 give the distribution of the effective plastic strain at different simulation time respectively. The reaction force and volume change during the simulation are plotted in Figures 12 and 13 respectively.

Acknowledgements

We would like to thank Dr. John Watton of Alcoa Technical Center for providing the test examples and helpful suggestions.

References

- [1] T. Belytschko, Y.Y. Lu and L. Gu, "Element-free Galerkin methods," *Int. J. Numer. Methods Engrg.* 37 (1994) 229-256.
- [2] B. Boroomand, and O.C. Zienkiewicz, "Recovery Procedures in Error Estimation and Adaptivity. Part II: Adaptivity in Nonlinear Problems of Elasto-Plasticity Behaviour", *Computer Methods in Applied Mechanics and Engineering*, Vol. 176, 127-146, 1999.
- [3] J. S. Chen, C. Pan, C. T. Wu and W. K. Liu, "Reproducing Kernel Particle Methods to Large Deformation Analysis of Nonlinear Structures," *Computer Methods in Applied Mechanics and Engineering*, Vol. 139, p. 195-227, 1996.
- [4] Chen, J. S., Han, W., You, Y., Meng, X "A Reproducing Kernel Method with Nodal Interpolation Property," *Int. J. Journal for Numerical Methods in Engineering*, Vol. 56, (2003) 935-960.
- [5] N. S. Lee and K. J. Bathe, Error Indicators and Adaptive Remeshing in Large Deformation Finite Element Analysis, *Finite Elem. Anal. Des.* 16 (1994) 99-139
- [6] S. Li and W. K. Liu, "Meshfree and Particle Methods and Their Applications," *Applied Mechanics Review*, Vol. 55, pages 1-34, 2002.
- [7] W. K. Liu, W. Han, H. Lu and S. Li, Reproducing Kernel Element Method, Part I Theoretical Formulation, *Comp. Methods in Applied Mechanics and Engineering*, 193: 933–951, 2004.
- [8] W. K. Liu, S. Jun, and Y. F. Zhang, "Reproducing Kernel Particle Method", *Int. J. Numer. Methods Fluids*, 20 (1995) 1081-1106.
- [9] H. Lu, and J. S. Chen, "Adaptive Meshfree Particle Method," *Lecture Notes in Computational Science and Engineering*, Vol. 26, pp. 251-267, 2002.
- [10] M. Ortiz and J.J. Quigley, IV, "Adaptive Mesh Refinement in Strain Localization Problems", *Comp. Methods in Applied Mechanics and Engineering*, 90, 781–804, 1991.
- [11] D. Peric, Ch. Hochard, M. Dutko, and D.R.J. Owen, "Transfer Operators for Evolving Meshes in Small Strain Elasto-Plasticity", *Comp. Methods in Appl. Meh. Engrg.*, 137, 331–344, 1996.
- [12] J. -P. Ponthot, T. Belytschko, "Arbitrary Lagrangian-Eulerian Formulation for Element-Free Galerkin Method", *Comp. Meths. in Applied Mechanics and Engineering*, 152, 19–46, 1998
- [13] T. Rabczuk, T. Belytschko, "Adaptivity for structured meshfree particle methods in 2D and 3D," *International Journal for Numerical Methods in Engineering*, Vol. 63, p. 1559-1582, 2005.
- [14] C.A. Duarte, and J.T. Oden, "An hp adaptive method using clouds", *Comp. Methods in Appl. Meh. Engrg.*, 139, 237-262, 1996.
- [15] J.M. Melenk, and I. Babuska, "The Partition of Unity Method", *Comp. Methods in Appl. Meh. Engrg.*, 139, 289-314, 1996.